Report

Current Biology

Engram stability and maturation during systems consolidation

Graphical abstract

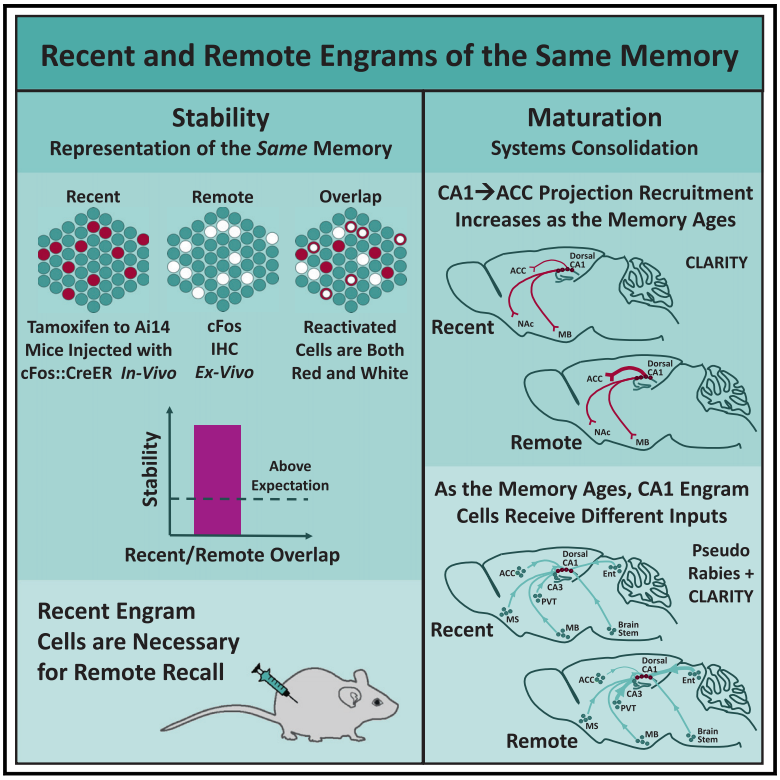

Highlights

- CA1 engrams of the same memory remain stable between recent and remote recalls
- Inhibition of recent recall engram cells during remote recall impairs memory
- We employed CLARITY with c-Fos::CreER, retro-AAV, and pseudo-rabies for circuit mapping
- New cells are added to CA1 remote engram based on anterograde/retrograde connections

Authors

Ron Refaeli, Tirzah Kreisel, Maya Groysman, Adar Adamsky, Inbal Goshen

Correspondence

inbal.goshen@elsc.huji.ac.il

In brief

Refaeli et al. investigate recent and remote CA1 engrams of the same memory and find them to remain stable. Furthermore, inhibition of recent recall engram cells during remote recall impairs memory. On the other hand, new cells are added to the CA1 remote engram during maturation based on their anterograde and retrograde connections.

Refaeli et al., 2023, Current Biology *33*, 3942–3950
September 25, 2023
https://doi.org/10.1016/j.cub.2023.07.042

CellPress

CellPress
OPEN ACCESS

Current Biology

Report

Engram stability and maturation during systems consolidation

Ron Refaeli,[1] Tirzah Kreisel,[1] Maya Groysman,[2] Adar Adamsky,[1] and Inbal Goshen[1,3,4,*]
[1]Edmond and Lily Safra Center for Brain Sciences (ELSC), The Hebrew University of Jerusalem, Jerusalem 91904, Israel
[2]ELSC Vector Core Facility, The Hebrew University of Jerusalem, Jerusalem 91904, Israel
[3]Twitter: @GoshenInbal
[4]Lead contact
*Correspondence: inbal.goshen@elsc.huji.ac.il
https://doi.org/10.1016/j.cub.2023.07.042

SUMMARY

Remote memories play an important role in how we perceive the world, and they are rooted throughout the brain in "engrams": ensembles of cells that are formed during acquisition. Upon their reactivation, a specific memory can be recalled.[1–12] Many studies have focused on the ensembles in CA1 of the hippocampus and the anterior cingulate cortex (ACC). However, the evolution of these components during systems' consolidation has not yet been comprehensively addressed.[13–16] By applying transgenic approaches for ensemble identification, CLARITY, retro-AAV, and pseudo-rabies virus for circuit mapping, and chemogenetics for functional interrogation, we addressed the dynamics of recent and remote CA1 ensembles. We expected both stability (as they represent the same memory) and maturation (over time). Indeed, we found that CA1 engrams remain stable between recent and remote recalls, and the inhibition of engrams for recent recall during remote recall functionally impairs memory. We also found that new cells in the remote recall engram in the CA1 are not added randomly during maturation but differ according to their connections. First, we show in two ways that the anterograde CA1 → ACC engram cell projection grows larger. Finally, in the retrograde projections, the ACC reduces input to CA1 engram cells, whereas input from the entorhinal cortex and paraventricular nucleus of the thalamus increases. Our results shine fresh light on systems' consolidation by providing a deeper understanding of engram stability and maturation in the transition from recent to remote memory.

RESULTS AND DISCUSSION

What are the similarities between engrams of the same memory in sequential recalls? Previous studies examined only the overlap between the acquisition engram with recent or remote recall engrams and showed that there is a significant reactivation.[17–19] Some studies manipulated the activity of acquisition ensembles to show their necessity for memory (e.g., Ramirez et al.,[6] Kitamura et al.,[18] Tanaka et al.,[20] Liu et al.,[21] and de Sousa et al.[22]), while one study showed that the engram in PFCx is preserved from recent to remote memory.[23] It is unknown, however, whether the hippocampal neurons active during remote recall are the same cells active during recent recall, or whether both populations partially overlap with the acquisition engram cells but not with one another.

Studying the stability of memory engrams requires double labeling of cell activity within the same animal more than once during a memory-related task. One approach is targeting immediate-early genes, since their transcription occurs when a neuron is hyper-activated (e.g., if it is involved in a specific memory) and because they can be tagged at a specific time window while the animal remains unharmed.[24] To tag memory engrams, we injected AAV5-c-Fos-CreER, inducing the expression of Cre under the promoter of the immediate early gene c-Fos[19,24,25] (which is elevated in active neurons) to the dorsal-CA1 (dCA1) of Ai14-reporter mice (129S6-Gt(ROSA) 26Sor$^{tm14(CAG-tdTomato)Hze}$; STAR Methods), conditionally expressing tdTomato in cells that express Cre. The activity of Cre on tdTomato is limited to a 4–8 h time window,[26] defined by injection of 4-hydroxytamoxifen (4-OHT) (25 mg/kg, intraperitoneally [i.p.]), allowing CRE translocation into the nucleus and consequently tdTomato expression (Figures 1A and 1B). Three weeks after viral injection, mice underwent fear conditioning training, in which a foot shock was paired with a novel context, and recall was assessed at the recent (2 days) or remote (28 days) time period. At both points, the mice exhibit increased freezing compared with acquisition ($F_{2,18}$ = 17.65, p = 0.000057) (Figure 1C). A separate group of mice did not undergo fear conditioning and were only exposed to their home cage as a control. Animals were injected with 4-OHT 60 min after the relevant behavior in order to fluorescently tag all active cells during that task. We found that during memory acquisition and recent or remote recall, 4-OHT introduction caused 16.89%, 18.57%, and 14.65% (respectively) of the CA1 cells to express c-Fos, whereas in control mice (which remained in their home cage), only 11.22% of the cells were active ($F_{3,41}$ = 2.87, p = 0.048) (Figure S1A). To tag the active cells in two engrams of the same memory in the same animals, the earlier time point was tagged in red (tdTomato) using the 4-OHT to

CellPress
OPEN ACCESS

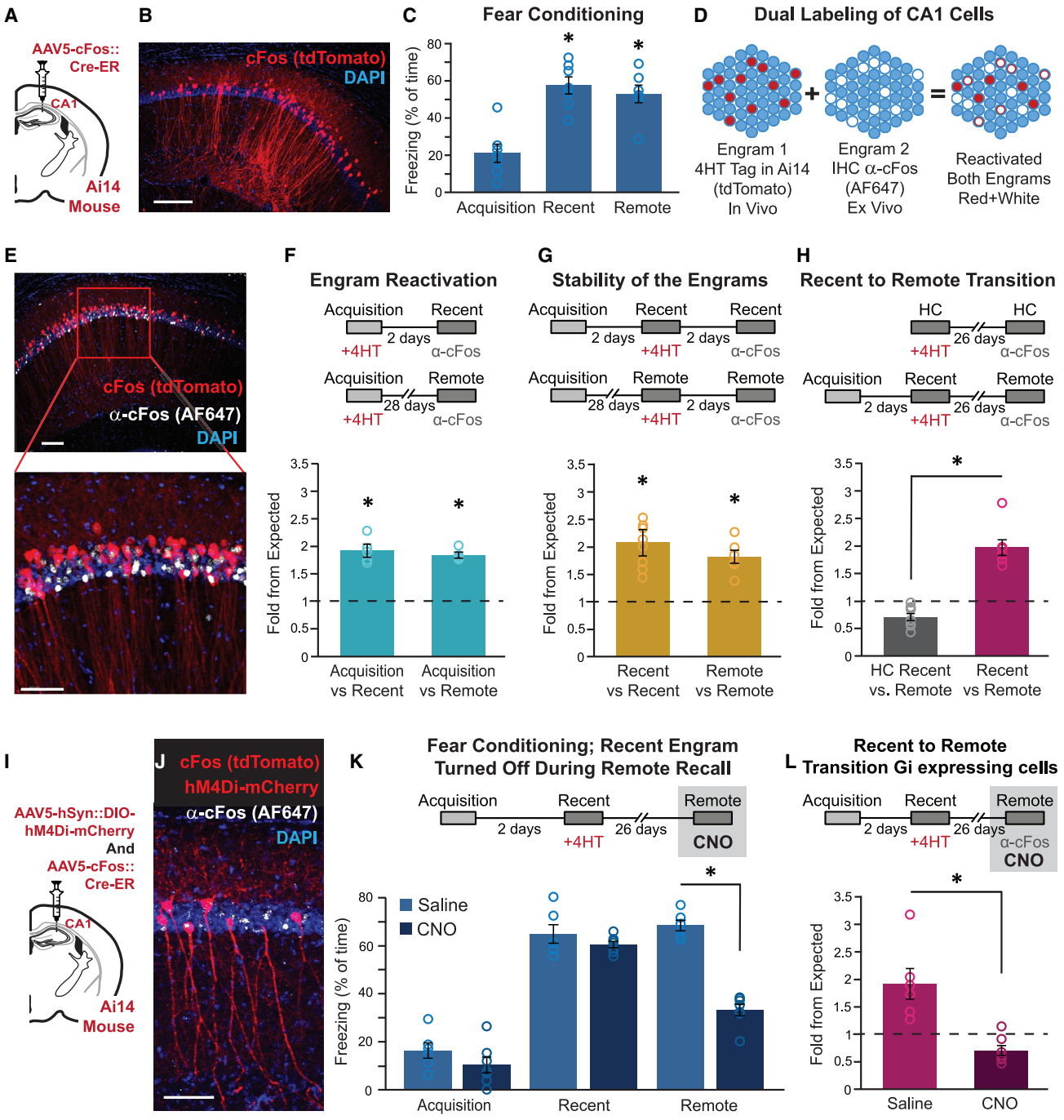

Figure 1. CA1 engram neurons are stable across recent and remote memory transition, and the recent ensemble is crucial for remote recall

(A) Ai14 mice were injected with a c-Fos-CreER vector into the dorsal-CA1.

(B) Cells that were active and thus expressed c-Fos during 4-OHT administration express tdTomato (red). Scale bars, 100 μm.

(C) Mice performance during fear conditioning paradigm (n = 7). Freezing is apparent at both the recent and the remote time points (acquisition-recent, p = 0.0001; acquisition-remote, p = 0.00043).

(D and E) Dual labeling of c-Fos in the CA1. tdTomato (red) in cells from the first time point and α-c-Fos IHC (AF647, white) in all c-Fos-positive cells during the second time point. Reactivated cells are both red and white. Scale bars, 50 μm.

(F) Reactivation of the acquisition tdTomato-positive cells (tagged first with 4-OHT) during both recent (n = 5) and remote (n = 5) recall (tagged second with α-c-Fos IHC). The acquisition engram cells are significantly reactivated (p = 0.001 and p = 0.000088).

(G) Stability of the engram cells 2 days apart during both recent (n = 10) and remote (n = 6). There was significant stability at both time points (p = 0.001 and p = 0.001).

(legend continued on next page)

Ai14+c-Fos-creER as explained above (1st tag, *in vivo*), and the later time point was tagged in far-red (Alexa Fluor 647) by IHC against the c-Fos protein (2nd tag, *ex vivo*). Reactivated cells are both tagged in red and stained white (Figures 1D and 1E).

First, we investigated the reactivation of acquisition of CA1 engram cells during recent or remote memory recall. As shown in previous studies,[17,18] reactivation of the CA1 acquisition engram exceeded chance levels in both recent and remote recall (see quantification and statistical analysis in the STAR Methods). Specifically, we found the overlap between acquisition and recent recall to be 192% of the expected and that of acquisition and remote recalls to be 183% ($t_{(4)}$ = 10.032, p = 0.001; $t_{(4)}$ = 16.042, p = 0.000088, respectively) with no difference between them (p > 0.45) (Figures 1F, S1B, and S1C). Next, for the first time, we checked the stability of the engram within recent or remote memory twice with 2 days between each examination. One group of mice was fear conditioned and tested for recent recall 2 days later and again on day 4, whereas a second group of mice was fear conditioned and tested for remote recall on day 28 and then again on day 30 (Figures S1D and S1E). The time interval between the c-Fos tagging with 4-OHT to the IHC labeling was 2 days, allowing enough time for the 4-OHT to clear from the body. We found that the stability of engram activation over 2 days during both recent and remote recalls was high (207% and 182% of chance level, $t_{(9)}$ = 4.69, p = 0.001 and $t_{(5)}$ = 6.38, p = 0.001, respectively) (Figure 1G). Finally, we examined whether there exists an overlap between recent and remote engrams, as past research only showed the overlap of each to acquisition individually.[17] We found that the overlap of c-Fos-labeled cells during recent and remote recall was significantly high (197% of chance level; t test; $t_{(6)}$ = 6.78, p = 0.001), as opposed to home cage mice that were tagged at the same intervals without a memory task performance and displayed lower reactivation than expected (t test; $t_{(8)}$ = 3.7, p = 0.006). These groups significantly differ from one another (71% of chance level; $t_{(14)}$ = 8.846, p = 4.1725E−7) (Figures 1H and S1F). When calculating the ratio of c-Fos staining-tagged engram cells who were NOT tagged *in vivo* with tdTomato (c-Fos+tdTomato−), no differences from what was expected were found for any of the groups discussed so far (Figure S1G).

The significant overlap between recent and remote engrams raises the question of how turning off the recent engram during remote recall will affect remote memory. To test this question, we injected Ai14 mice with AAV5-hSyn::DIO-hM4Di-mCherry and AAV5-c-Fos::Cre-ER (Figure 1I), together allowing the induction of hM4Di chemogenetic inhibitor (and tdTomato) only in cells that expressed c-Fos during 4-OHT injection in recent recall (Figure 1J). Since tdTomato and mCherry are both red, we performed IHC staining against mCherry and found high penetrance, with 95.86% ± 1.51% of active cells during recent recall (tdTomato) also expressing hM4Di (mCherry) (Figure S1H), compared with 36.96% ± 3.2% when no hM4Di-mCherry is present. 30 min before remote recall, we administered clozapine *N*-oxide (CNO) (10 mg/kg, i.p.), thus inhibiting the recent engram cells prior to the task and preventing their reactivation. Animals treated with CNO during remote recall showed a dramatic impairment in memory retrieval compared with saline-injected controls (t test; $t_{(11)}$ = 10.655, p = 3.9E−7) (Figure 1K). The percent of c-Fos tdTomato+ cells from the CA1 pyramidal layer cells during recent recall was similar across saline and CNO groups, but during remote recall (the time of CNO administration), the CNO-injected mice showed fewer c-Fos+ cells (t test; $t_{(11)}$ = 5.96, p = 9.5E−5) (Figure S1I). Although the overlap of c-Fos labeling during recent and remote recall was significantly higher in saline-injected mice (192% of chance level; t test; $t_{(5)}$ = 3.579 p = 0.016), CNO-injected animals showed a decrease from chance level (t test; $t_{(6)}$ = 3.266, p = 0.017), with a significant difference between the groups (t test; $t_{(11)}$ = 4.143, p = 0.001) (Figures 1L and S1J).

When calculating the ratio of c-Fos staining-tagged remote engram cells who were NOT tagged *in vivo* with tdTomato during recent recall, we again found no differences from what was expected (Figure S1K). Finally, to make sure that a random group of cells would not result in a similar effect, we tagged with c-Fos::Cre-ER and hM4Di-mCherry mice during their time in the home cage and treated them with either CNO (n = 8) or saline (n = 5). No effect on freezing behavior was found during acquisition or remote recall upon CNO application (Figure S1L), and the overlap of c-Fos-labeled cells during recent and remote recall was unaltered in both CNO and saline groups in home cage-tagged mice, and they did not differ from one another (Figure S1M).

Our results support the well-known fact that CA1 is necessary for memory acquisition and recent recall,[27,28] as well as the still controversial notion that the CA1 is involved in remote recall.[29–31] Recent and remote recall engrams both involve reactivation of the cells that were active during the acquisition of the memory as previously shown[17,18]; they are stable over a 2-day period, and most importantly, the engrams overlap during the transition between recent and remote recall.

A former study showed that activating the acquisition ensemble in mPFC enhances remote memory, whereas inhibiting it impairs remote recall.[32] Another experiment targeted the remote engram and showed that it enhances extinction when activated and reduces extinction when inactivated.[33] We showed that the overlap in CA1 is functionally important and that the remote engram relies on the recent engram (but not on a random group of cells), since preventing the recent recall engram from reactivation during remote memory impairs recall.

(H) Comparing recent and remote CA1 engram cells. The ensembles are stable during the transition from recent to remote memory (n = 7), compared with home caged controls (n = 9) (p = 4.1725E−7).
(I) Ai14 mice were injected, like before, with a c-Fos-CreER vector and also with hM4Di-mCherry into the dorsal-CA1.
(J) Double labeling of c-Fos-tdTomato+ cells and hM4Di-mCherry in the recent engram, and α-c-Fos after remote recall. Scale bars, 50 μm.
(K) Behavioral performance of the hM4Di expressing mice treated with either CNO or saline (CNO, n = 7; saline, n = 6). Significant reduction in freezing behavior is apparent during remote recall when CNO is applied (p = 3.9E−7).
(L) Recent to remote transition reactivation is reduced when CNO is applied, compared with saline (CNO, n = 7; saline, n = 6) (p = 0.001). Data presented as mean ± SEM.
See also Figure S1.

CellPress
OPEN ACCESS

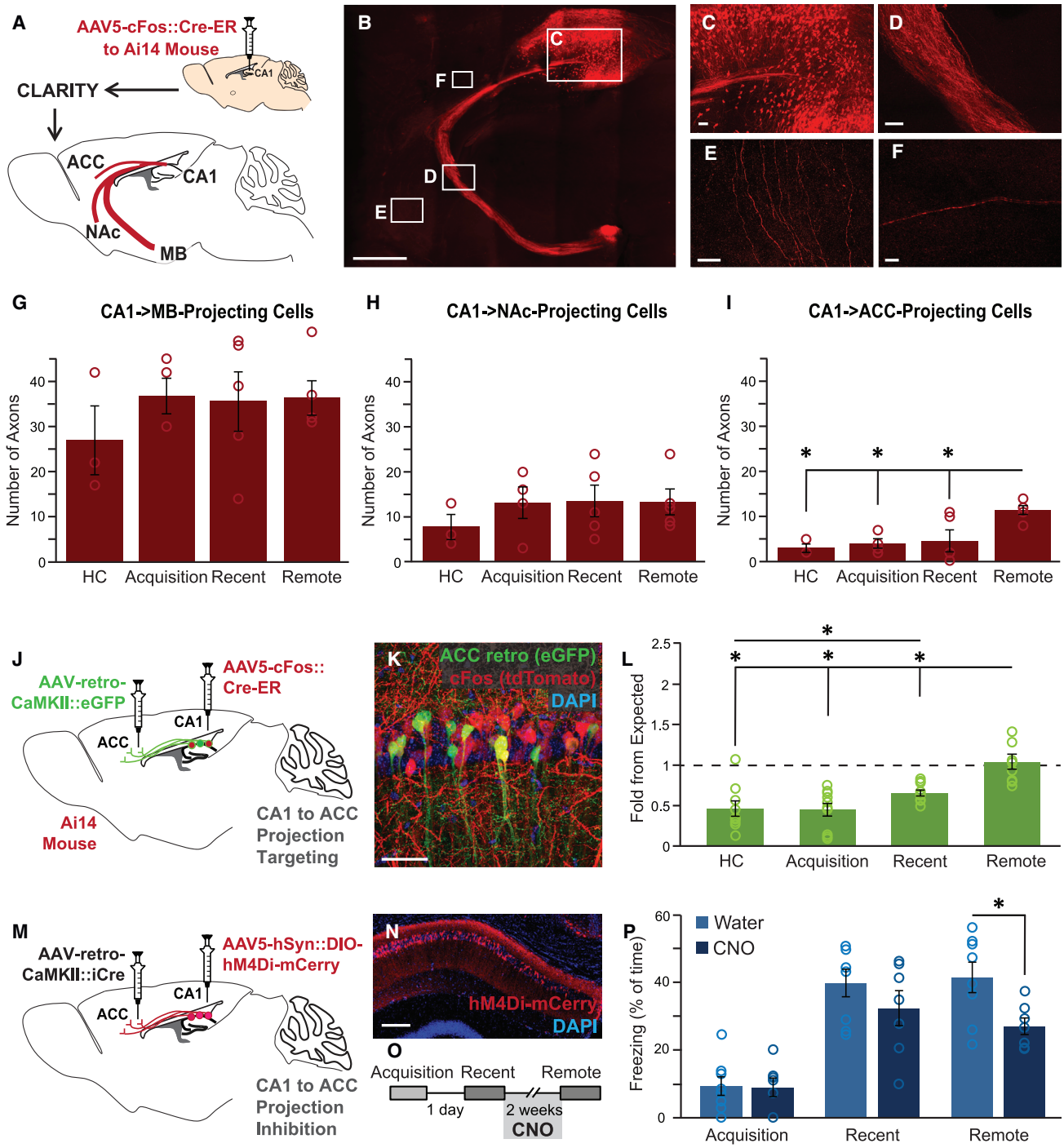

Figure 2. CA1 → ACC-projecting cell recruitment increases with memory maturation

(A) Ai14 mice were injected with a c-Fos-CreER vector into the CA1 to tag active cells. CLARITY procedure allowing full brain imaging was performed at the different memory stages.

(B) An entire hemisphere of a mouse expressing tdTomato (red) in c-Fos-positive cells. Scale bars, 1 mm.

(C–F) Zoomed-in images of the CA1 engram cell bodies. Scale bars, 10 μm. (C) The fornix going toward the MB, (D) the axons projecting toward the NAc, (E), and the projection toward the ACC (F).

(G–I) The number of tdTomato-positive axons counted at the different memory stages (n = 3–5/group) going toward the MB ($p = 0.661$) (G), the NAc ($p = 0.664$) (H), or the ACC (I). Only in this region, the remote recall projection size is double that of the other time points (HC-remote, $p = 0.026$; acquisition-remote, $p = 0.033$; recent-remote, $p = 0.039$).

(J) Ai14 mice were injected with a c-Fos-CreER vector to tag active cells in the CA1 and AAV-retro-CaMKII::eGFP into the ACC to tag cells in CA1 projecting to the ACC (CA1 → ACC).

(legend continued on next page)

When investigating changes in recent versus remote recall engrams, understanding the dynamics in the long-range connections between different brain regions is essential. Anatomically, the connections between two different brain structures do not alter, but the selection of cells within each structure comprising an engram can certainly change, which may be due to their specific projection target. Targeting the anterograde connections of the hippocampal engram neurons at different time points can reveal the dynamic relations with their downstream brain structures. These connections were imaged in whole clear brains by CLARITY.[26,34,35] We first quantified the distribution of dCA1 active cell projections throughout the entire brain by tagging the active cells as we did before: Ai14 mice injected with c-Fos::Cre-ER and then administered 4-OHT 1 h after the time of behavior. Four weeks after tagging the active cells, mice were sacrificed, and a CLARITY[26] procedure was performed in order to turn the brains transparent, allowing imaging of full hemispheres with single-axon resolution (Figure 2A; Video S1). The dCA1 projects to several targets, and three of them are clearly visible: the largest projection reaches the mammillary bodies (MBs), the second reaches the nucleus accumbens (NAc), and the smallest projections reach the ACC (Figures 2B–2F). For all behavioral groups of mice, we found the same total number of axons projecting from the dCA1 engram cells (Figure S2A). We found no significant changes in the number of axons or the percent of axons from total throughout the memory progression in the MB ($p > 0.661$) or the NAc ($p > 0.664$) (Figures 2G, 2H, S2B, and S2C). The ACC paints a different picture entirely: in home cage, acquisition, and recent recall, only a small portion of the axons from c-Fos tdTomato+ cells head toward the ACC, whereas during remote recall, the portion of active cells in the CA1 that send their axons toward the ACC doubles ($F_{3,13} = 5.42$, $p = 0.012$) (Figures 2I and S2D).

In light of these findings, and past research suggesting a role for ACC in remote memory,[15,29,36–42] we injected a c-Fos::Cre-ER to the ACC in Ai14 mice (Figure S2E) to observe the levels of engram reactivation in ACC for all five different comparisons that we formerly made in the CA1 (Figures 1F–1H). We found no overlap between acquisition and recent or remote recall (Figure S2F) on one hand but observed stable engram activation over 2 days during both recent and remote recalls (186% and 188% of chance level, $t_{(9)} = 4.496$, $p = 0.0015$ and $t_{(5)} = 3.307$, $p = 0.021$, respectively) (Figure S2G). Then, we examined the overlap between recent and remote engrams and found that in the ACC as well, the overlap of c-Fos-labeled cells during recent and remote recall was significantly high (158% of chance level; t test; $t_{(14)} = 4.555$, $p = 0.0045$) (Figure S2H).

To further probe our observations, we injected a retrograde virus (AAVretro-CaMKII-eGFP) into the ACC to target the sub-population of neurons within the dCA1 that sends their projections toward the ACC (CA1 → ACC) and counted all infected cells in the CA1. In the same mice, c-Fos expression (tdTomato) during recent or remote recall was labeled as before (Figures 2J and 2K), and the mice underwent fear conditioning (Figure S2I). The likelihood of activation in the sub-population of CA1 → ACC increased as the memory aged ($F_{3,33} = 7.9$, $p = 0.000021$) (Figure 2L). However, even at its highest, it reached only the expected value in remote recall and was significantly lower than that expected for home cage, acquisition, and recent recall.

We previously showed that inhibiting the CA1 → ACC projection during acquisition impairs remote memory.[43] To check the functional significance of the CA1 → ACC projection in the transition from recent to remote memory, we injected wild-type mice with AAVretro:CaMKII-iCre in the ACC and AAV5-hSyn:DIO-hM4Di-mCherry in the CA1, thus enabling specific inhibition of the CA1 → ACC neurons (Figures 2M and 2N). The mice underwent fear conditioning acquisition, performed recent memory recall, and were then administered CNO via their drinking water for 2 weeks (10 mg/kg/day) before remote recall (Figure 2O). Remote recall was reduced in the CNO group compared with the controls that received water (t test; $t_{(13)} = 2.7$, $p = 0.018$) (Figure 2P), along with a significant reduction in c-Fos (Figures S2J and S2K).

Finally, we labeled dCA1 → NAc cells in a different group of mice by infecting the NAc with the same retrograde virus (Figures S2L and S2M). The mice underwent fear conditioning (Figure S2N), and the likelihood of activation within the sub-population of CA1 → NAc-projecting cells did not differ between recent and remote recall (Figure S2O).

Our results reveal that the projection of dCA1 engram cells to the ACC increases as the memory ages, i.e., that new neurons joining the remote engram are more likely to be ACC-projecting neurons. This does not indicate that the overall communication between the cells of two structures increases, only that a greater portion of these cells take part in the engram. Recent studies have shown the significance of the hippocampus not only during recent recall but also after systems consolidation as well,[29] which sits well with its increased connection to the ACC. Finally, we showed that CA1 → ACC cells are functionally involved, as remote memory recall is impaired if the projection is inhibited during systems' consolidation between recent and remote recall.

The hippocampus receives and integrates input from multiple brain structures. To investigate the input sources of the CA1 ensemble cells, i.e., which cells impinge upon them during the different stages of memory, we used the pseudo-rabies

(K) CA1 → ACC cells express eGFP (green) and the active c-Fos positive cells express tdTomato (red). Scale bars, 50 μm.
(L) The level of CA1 → ACC neurons participating in the engram increases as the memory ages (HC-remote, $p = 0.00016$; acquisition-remote, $p = 0.000031$; recent-remote, $p = 0.000653$).
(M) AAV-retro-CaMKII::iCre was injected in the ACC, and the Cre-dependent hM4Di-mCherry virus was injected into the CA1, and tagged only CA1 → ACC neurons.
(N) hM4Di (mCherry) CA1 → ACC cells in the CA1. Scale bars, 100 μm.
(O) Behavioral paradigm. Mice were continuously exposed to CNO between recent and remote recall to inhibit CA1 → ACC cells during systems consolidation.
(P) Memory performance was impaired in the CNO group ($n = 7$) where the CA1 → ACC cells were chronically inhibited, compared with the water control group ($n = 8$) ($p = 0.018$). Data presented as mean ± SEM.
See also Figure S2 and Video S1.

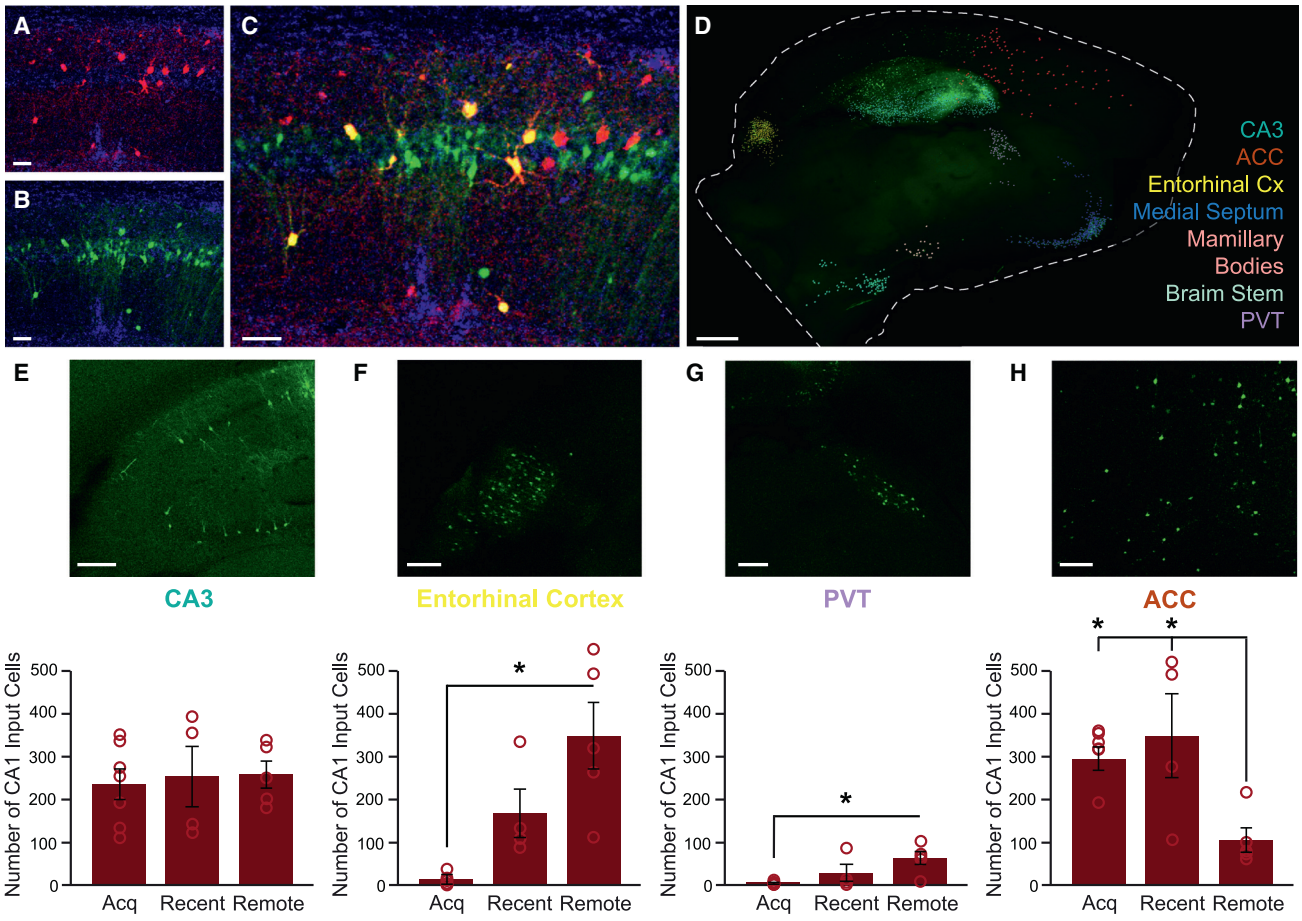

Figure 3. CA1 engram cells receive different brain-wide input as the memory ages

(A) CA1 engram cells express TVA-mCherry (red). Scale bars, 50 μm.

(B) CA1 cells infected with pseudo-rabies vector express YFP (green). Scale bars, 50 μm.

(C) Overlay of (A) and (B), showing cells that express both mCherry and YFP (43% of mCherry+ cells) are considered starting cells. Scale bars, 50 μm.

(D) Whole-brain imaging reveals seven brain structures with input cells to the CA1 engram cells. Scale bars, 1 mm.

(E–H) Top: input cells in TRAP mice cleared brains. Bottom: number of input cells counted during the different memory stages (acquisition, n = 7; recent, n = 4; remote, n = 5). Scale bars, 100 μm. The number stayed the same in the CA3 ($p = 0.92$) (E), increased in the entorhinal cortex (acquisition-remote, $p = 0.0006$) (F) and the PVT (acquisition-remote, $p = 0.007$) (G), and reduced in the ACC (acquisition-remote, $p = 0.007$; recent-remote, $p = 0.016$) and (H) as the memory matures. Data presented as mean ± SEM.

See also Figure S3 and Video S2.

approach that can leap back from the expressing neurons to their pre-synaptic cells.[44] It was used for a different purpose in the CA1[45] and was recently used to study recent memory in the amygdala[46]: we first expressed the mutated avian tumor virus (TVA) receptor (TC66T) and glycoprotein (oPBG) in ensemble cells by injecting AAV2-CAG-flex-TC66T-mCherry and AAV2-CAG-flex-oPBG into the dCA1 of TRAP2 mice ($Fos^{tm2.1(icre/ERT2)Luo}$) expressing CreER protein under the c-Fos promoter. Three weeks later, mice underwent a fear conditioning task, and 4-OHT was introduced during either acquisition, recent, or remote recall, allowing the Cre to enter the nucleus in the active ensemble cells and induce the expression of TVA and the glycoprotein (Figure 3A). Two weeks later, a pseudo-rabies virus (ENV-Rb-ΔG-eYFP) was injected into the same location in the hippocampus, and it infected and complemented only in the cells expressing TC66T + GP, i.e., those that are a part of the ensemble cells (Figures 3B and 3C) and spread to their pre-synaptic neurons. After another week, the mice were sacrificed, and the brains were clarified. We then imaged and analyzed the spatial distribution of the presynaptic cells throughout the entire brain (Figure 3D; Video S2) at the acquisition, recent, and remote recall time points (fear condition: $t_{(12)} = 16.44$, $p = 0.00028$; $t_{(6)} = 4.72$, $p = 0.0033$; and $t_{(8)} = 7.27$, $p = 0.000086$, respectively) (Figures S3A–S3C). We located seven different main brain structures that send their projections toward the dCA1 engram cells and counted the number of cells at each memory stage. Notably, we found that the total number of input cells to the CA1 engram remains similar across acquisition, recent, and remote recall (1,298, 1,273, and 1,200 input cells, respectively) (Figure S3D). As expected, CA3, a main projection to the CA1, did not change the number of its input cells into the CA1 engram over time (Figure 3E). The lateral and medial entorhinal cortices (major cortical

inputs to the hippocampus known to play a role in both recent and remote memory[47–50]) and the paraventricular thalamus (PVT; stress-related nucleus known to affect auditory cued memory[51,52]) increase their number of input cells to dCA1 during remote recall ($F_{2,13}$ = 13.02, p = 0.0008; $F_{2,13}$ = 6.9, p = 0.009, respectively) (Figures 3F and 3G). On the other hand, the ACC decreases the number of input cells into the CA1 during remote recall ($F_{2,13}$ = 6.33, p = 0.012) (Figure 3H). In the medial septum, during remote recall, the number of input cells projecting to the CA1 engram decreases, but no difference was found between recent and remote recall ($F_{2,13}$ = 4.14, p = 0.041) (Figure S3E), and no change in the number of input cells at different time points in either the MB or brain stem was observed (Figures S3F and S3G).

These results provide a comprehensive view of the CA1 engram brain-wide connectivity at different memory stages. It seems that the addition of new cells to the remote ensemble in the CA1 is positively biased in favor of cells with input from the entorhinal cortices and the PVT as opposed to cells receiving input from the ACC.

Remote memories are harder to extinguish than recent ones,[53] and the similarity between ensembles of two memories is higher when they are formed hours apart compared with a week apart[54]; therefore, we hypothesize that this memory permanency is based on increased ensemble stability, and indeed, the CA1 engram remains relatively similar between recent and remote memory and is functionally critical for remote memory. However, new neurons still join the remote ensemble, and our findings of changed anterograde and retrograde projections can only stem from the new cells that join the remote engram and constitute the changes from the recent engram. These findings shed light on the transition from recent to remote memory and the remote ensemble selection mechanisms and bring us closer to understanding the process of systems consolidation.

STAR★METHODS

Detailed methods are provided in the online version of this paper and include the following:

- KEY RESOURCES TABLE
- RESOURCE AVAILABILITY
  - Lead contact
  - Material availability
  - Data and code availability
- EXPERIMENTAL MODEL AND STUDY PARTICIPANT DETAILS
- METHOD DETAILS
  - Stereotactic Injections
  - Viral Vectors
  - 4-hydroxytamoxifen (4-OHT)
  - CNO administration
  - Fear Conditioning
  - Immunohistochemistry
  - CLARITY
  - Confocal Imaging
  - Imaris analysis
- QUANTIFICATION AND STATISTICAL ANALYSIS

SUPPLEMENTAL INFORMATION

Supplemental information can be found online at https://doi.org/10.1016/j.cub.2023.07.042.

ACKNOWLEDGMENTS

We thank the entire Goshen lab for their support. This project has received funding from the European Research Council (ERC) under the European Union's Horizon 2020 research and innovation program (grant agreement no. 803589), the Israel Science Foundation (ISF grant no. 1815/18), and the Canada-Israel grants (CIHR-ISF, grant no. 2591/18). We thank Ami Citri, Mickey London, Adi Doron, Lior Naggan, and Yael Morose for the critical reading of the manuscript. This work is dedicated to the memory of Mrs. Lily Safra, a great supporter of brain research.

AUTHOR CONTRIBUTIONS

R.R. performed all engram experiments. T.K. contributed to injections, histology, and behavior. A.A. performed the non-engram CA1 → ACC projection experiment. M.G. produced viral vectors. I.G. conceived and supervised all aspects of the project and wrote the manuscript with input from R.R. and T.K.

DECLARATION OF INTERESTS

The authors declare no competing interests.

INCLUSION AND DIVERSITY

We support inclusive, diverse, and equitable conduct of research.

Received: May 12, 2023
Revised: June 27, 2023
Accepted: July 20, 2023
Published: August 15, 2023

REFERENCES

1. Josselyn, S.A., Köhler, S., and Frankland, P.W. (2017). Heroes of the engram. J. Neurosci. *37*, 4647–4657.
2. Josselyn, S.A., and Tonegawa, S. (2020). Memory engrams: recalling the past and imagining the future. Science *367*, eaaw4325.
3. Tonegawa, S., Liu, X., Ramirez, S., and Redondo, R. (2015). Memory engram cells have come of age. Neuron *87*, 918–931.
4. Ryan, T.J., Roy, D.S., Pignatelli, M., Arons, A., and Tonegawa, S. (2015). Memory. Engram cells retain memory under retrograde amnesia. Science *348*, 1007–1013.
5. Reijmers, L.G., Perkins, B.L., Matsuo, N., and Mayford, M. (2007). Localization of a stable neural correlate of associative memory. Science *317*, 1230–1233.
6. Ramirez, S., Liu, X., Lin, P.A., Suh, J., Pignatelli, M., Redondo, R.L., Ryan, T.J., and Tonegawa, S. (2013). Creating a false memory in the hippocampus. Science *341*, 387–391.
7. Roy, D.S., Park, Y.G., Kim, M.E., Zhang, Y., Ogawa, S.K., DiNapoli, N., Gu, X., Cho, J.H., Choi, H., Kamentsky, L., et al. (2022). Brain-wide mapping reveals that engrams for a single memory are distributed across multiple brain regions. Nat. Commun. *13*, 1799.
8. Vetere, G., Kenney, J.W., Tran, L.M., Xia, F., Steadman, P.E., Parkinson, J., Josselyn, S.A., and Frankland, P.W. (2017). Chemogenetic interrogation of a brain-wide fear memory network in mice. Neuron *94*, 363–374.e4.
9. Tomé, D.F., Sadeh, S., and Clopath, C. (2022). Coordinated hippocampal-thalamic-cortical communication crucial for engram dynamics underneath systems consolidation. Nat. Commun. *13*, 840.
10. Lavi, A., Sehgal, M., de Sousa, A.F., Ter-Mkrtchyan, D., Sisan, F., Luchetti, A., Okabe, A., Bear, C., and Silva, A.J. (2023). Local memory allocation recruits memory ensembles across brain regions. Neuron *111*, 470–480.e5.

11. Mau, W., Morales-Rodriguez, D., Dong, Z., Pennington, Z.T., Francisco, T., Baxter, M.G., Shuman, T., and Cai, D.J. (2022). Ensemble remodeling supports memory-updating. Preprint at bioRxiv. https://doi.org/10.1101/2022.06.02.494530.
12. Tomé, D.F., Zhang, Y., Aida, T., Sadeh, S., Roy, D.S., and Clopath, C. (2022). Dynamic and selective engrams emerge with memory consolidation. Preprint at bioRxiv. https://doi.org/10.1101/2022.03.13.484167.
13. Abel, T., and Lattal, K.M. (2001). Molecular mechanisms of memory acquisition, consolidation and retrieval. Curr. Opin. Neurobiol. *11*, 180–187.
14. Matynia, A., Kushner, S.A., and Silva, A.J. (2002). Genetic approaches to molecular and cellular cognition: a focus on LTP and learning and memory. Annu. Rev. Genet. *36*, 687–720.
15. Frankland, P.W., and Bontempi, B. (2005). The organization of recent and remote memories. Nat. Rev. Neurosci. *6*, 119–130.
16. Squire, L.R., Genzel, L., Wixted, J.T., and Morris, R.G. (2015). Memory consolidation. Cold Spring Harb. Perspect. Biol. *7*, a021766.
17. Tayler, K.K., Tanaka, K.Z., Reijmers, L.G., and Wiltgen, B.J. (2013). Reactivation of neural ensembles during the retrieval of recent and remote memory. Curr. Biol. *23*, 99–106.
18. Kitamura, T., Ogawa, S.K., Roy, D.S., Okuyama, T., Morrissey, M.D., Smith, L.M., Redondo, R.L., and Tonegawa, S. (2017). Engrams and circuits crucial for systems consolidation of a memory. Science *356*, 73–78.
19. DeNardo, L.A., Liu, C.D., Allen, W.E., Adams, E.L., Friedmann, D., Fu, L., Guenthner, C.J., Tessier-Lavigne, M., and Luo, L. (2019). Temporal evolution of cortical ensembles promoting remote memory retrieval. Nat. Neurosci. *22*, 460–469.
20. Tanaka, K.Z., Pevzner, A., Hamidi, A.B., Nakazawa, Y., Graham, J., and Wiltgen, B.J. (2014). Cortical representations are reinstated by the hippocampus during memory retrieval. Neuron *84*, 347–354.
21. Liu, X., Ramirez, S., Pang, P.T., Puryear, C.B., Govindarajan, A., Deisseroth, K., and Tonegawa, S. (2012). Optogenetic stimulation of a hippocampal engram activates fear memory recall. Nature *484*, 381–385.
22. de Sousa, A.F., Cowansage, K.K., Zutshi, I., Cardozo, L.M., Yoo, E.J., Leutgeb, S., and Mayford, M. (2019). Optogenetic reactivation of memory ensembles in the retrosplenial cortex induces systems consolidation. Proc. Natl. Acad. Sci. USA *116*, 8576–8581.
23. Lee, J.H., Kim, W.B., Park, E.H., and Cho, J.H. (2023). Neocortical synaptic engrams for remote contextual memories. Nat. Neurosci. *26*, 259–273.
24. DeNardo, L., and Luo, L. (2017). Genetic strategies to access activated neurons. Curr. Opin. Neurobiol. *45*, 121–129.
25. Shpokayte, M., McKissick, O., Guan, X., Yuan, B., Rahsepar, B., Fernandez, F.R., Ruesch, E., Grella, S.L., White, J.A., Liu, X.S., and Ramirez, S. (2020). Hippocampal cells multiplex positive and negative engrams. Commun. Biol. *5*, 1009.
26. Ye, L., Allen, W.E., Thompson, K.R., Tian, Q., Hsueh, B., Ramakrishnan, C., Wang, A.C., Jennings, J.H., Adhikari, A., Halpern, C.H., et al. (2016). Wiring and molecular features of prefrontal ensembles representing distinct experiences. Cell *165*, 1776–1788.
27. Strekalova, T., Zörner, B., Zacher, C., Sadovska, G., Herdegen, T., and Gass, P. (2003). Memory retrieval after contextual fear conditioning induces c-Fos and JunB expression in CA1 hippocampus. Genes Brain Behav. *2*, 3–10.
28. Daumas, S., Halley, H., Francés, B., and Lassalle, J.M. (2005). Encoding, consolidation, and retrieval of contextual memory: differential involvement of dorsal CA3 and CA1 hippocampal subregions. Learn. Mem. *12*, 375–382.
29. Goshen, I., Brodsky, M., Prakash, R., Wallace, J., Gradinaru, V., Ramakrishnan, C., and Deisseroth, K. (2011). Dynamics of retrieval strategies for remote memories. Cell *147*, 678–689.
30. Wheeler, A.L., Teixeira, C.M., Wang, A.H., Xiong, X., Kovacevic, N., Lerch, J.P., McIntosh, A.R., Parkinson, J., and Frankland, P.W. (2013). Identification of a functional connectome for long-term fear memory in mice. PLoS Comput. Biol. *9*, e1002853.
31. Silva, B.A., Burns, A.M., and Gräff, J. (2019). A cFos activation map of remote fear memory attenuation. Psychopharmacol. (Berl.) *236*, 369–381.
32. Matos, M.R., Visser, E., Kramvis, I., van der Loo, R.J., Gebuis, T., Zalm, R., Rao-Ruiz, P., Mansvelder, H.D., Smit, A.B., and van den Oever, M.C. (2019). Memory strength gates the involvement of a CREB-dependent cortical fear engram in remote memory. Nat. Commun. *10*, 2315.
33. Khalaf, O., Resch, S., Dixsaut, L., Gorden, V., Glauser, L., and Gräff, J. (2018). Reactivation of recall-induced neurons contributes to remote fear memory attenuation. Science *360*, 1239–1242.
34. Chung, K., and Deisseroth, K. (2013). CLARITY for mapping the nervous system. Nat. Methods *10*, 508–513.
35. Willard, A.M., and Gittis, A.H. (2015). Mapping neural circuits with CLARITY. eLife *4*, e11409.
36. Anagnostaras, S.G., Maren, S., and Fanselow, M.S. (1999). Temporally graded retrograde amnesia of contextual fear after hippocampal damage in rats: within-subjects examination. J. Neurosci. *19*, 1106–1114.
37. Kitamura, T., Saitoh, Y., Takashima, N., Murayama, A., Niibori, Y., Ageta, H., Sekiguchi, M., Sugiyama, H., and Inokuchi, K. (2009). Adult neurogenesis modulates the hippocampus-dependent period of associative fear memory. Cell *139*, 814–827.
38. Maviel, T., Durkin, T.P., Menzaghi, F., and Bontempi, B. (2004). Sites of neocortical reorganization critical for remote spatial memory. Science *305*, 96–99.
39. Wiltgen, B.J., Brown, R.A., Talton, L.E., and Silva, A.J. (2004). New circuits for old memories: the role of the neocortex in consolidation. Neuron *44*, 101–108.
40. Frankland, P.W., Bontempi, B., Talton, L.E., Kaczmarek, L., and Silva, A.J. (2004). The involvement of the anterior cingulate cortex in remote contextual fear memory. Science *304*, 881–883.
41. Bontempi, B., Laurent-Demir, C., Destrade, C., and Jaffard, R. (1999). Time-dependent reorganization of brain circuitry underlying long-term memory storage. Nature *400*, 671–675.
42. Einarsson, E.Ö., and Nader, K. (2012). Involvement of the anterior cingulate cortex in formation, consolidation, and reconsolidation of recent and remote contextual fear memory. Learn. Mem. *19*, 449–452.
43. Kol, A., Adamsky, A., Groysman, M., Kreisel, T., London, M., and Goshen, I. (2020). Astrocytes contribute to remote memory formation by modulating hippocampal-cortical communication during learning. Nat. Neurosci. *23*, 1229–1239.
44. Wickersham, I.R., Lyon, D.C., Barnard, R.J., Mori, T., Finke, S., Conzelmann, K.K., Young, J.A., and Callaway, E.M. (2007). Monosynaptic restriction of transsynaptic tracing from single, genetically targeted neurons. Neuron *53*, 639–647.
45. Sun, Y., Nguyen, A.Q., Nguyen, J.P., Le, L., Saur, D., Choi, J., Callaway, E.M., and Xu, X. (2014). Cell-type-specific circuit connectivity of hippocampal CA1 revealed through Cre-dependent rabies tracing. Cell Rep. *7*, 269–280.
46. Lavi, A., Sehgal, M., Sisan, F., Okabe, A., Ter-Mkrtchyan, D., and Silva, A.J. (2021). A retrograde mechanism coordinates memory allocation across brain regions. Preprint at bioRxiv. https://doi.org/10.1101/2021.10.28.466361.
47. Eichenbaum, H., Sauvage, M., Fortin, N., Komorowski, R., and Lipton, P. (2012). Towards a functional organization of episodic memory in the medial temporal lobe. Neurosci. Biobehav. Rev. *36*, 1597–1608.
48. Sauvage, M.M., Beer, Z., Ekovich, M., Ho, L., and Eichenbaum, H. (2010). The caudal medial entorhinal cortex: a selective role in recollection-based recognition memory. J. Neurosci. *30*, 15695–15699.
49. Suh, J., Rivest, A.J., Nakashiba, T., Tominaga, T., and Tonegawa, S. (2011). Entorhinal cortex layer III input to the hippocampus is crucial for temporal association memory. Science *334*, 1415–1420.
50. Hales, J.B., Vincze, J.L., Reitz, N.T., Ocampo, A.C., Leutgeb, S., and Clark, R.E. (2018). Recent and remote retrograde memory deficit in rats

with medial entorhinal cortex lesions. Neurobiol. Learn. Mem. *155*, 157–163.

51. Do-Monte, F.H., Quiñones-Laracuente, K., and Quirk, G.J. (2015). A temporal shift in the circuits mediating retrieval of fear memory. Nature *519*, 460–463.
52. Choi, E.A., and McNally, G.P. (2017). Paraventricular thalamus balances danger and reward. J. Neurosci. *37*, 3018–3029.
53. Gräff, J., Joseph, N.F., Horn, M.E., Samiei, A., Meng, J., Seo, J., Rei, D., Bero, A.W., Phan, T.X., Wagner, F., et al. (2014). Epigenetic priming of memory updating during reconsolidation to attenuate remote fear memories. Cell *156*, 261–276.
54. Cai, D.J., Aharoni, D., Shuman, T., Shobe, J., Biane, J., Song, W., Wei, B., Veshkini, M., La-Vu, M., Lou, J., et al. (2016). A shared neural ensemble links distinct contextual memories encoded close in time. Nature *534*, 115–118.
55. Refaeli, R., Doron, A., Benmelech-Chovav, A., Groysman, M., Kreisel, T., Loewenstein, Y., and Goshen, I. (2021). Features of hippocampal astrocytic domains and their spatial relation to excitatory and inhibitory neurons. Glia *69*, 2378–2390.
56. Refaeli, R., and Goshen, I. (2022). Investigation of spatial interaction between astrocytes and neurons in cleared brains. J. Vis. Exp. https://doi.org/10.3791/63679.

STAR★METHODS

KEY RESOURCES TABLE

REAGENT or RESOURCE	SOURCE	IDENTIFIER
Antibodies		
rabbit anti-cFos	Synaptic Systems	Cat#226 003; RRID:AB_2231974
rabbit anti-mCherry	Invitrogen	#PA5-34974; RRID:AB_11399967
Alexa fluor 647 donkey anti rabbit	Jackson laboratory	#711-605-152; RRID:AB_2492288
Bacterial and virus strains		
AAV5-cFos::cre^{ER}	ELSC Vector Core Facility	N/A
AAVretro-CaMKII::iCre	ELSC Vector Core Facility	N/A
AAVretro-CaMKII::GFP	ELSC Vector Core Facility	N/A
AAV2-CAG::flex-TC66T-mCherry	ELSC Vector Core Facility	N/A
AAV2-CAG::flex-oPBG	ELSC Vector Core Facility	N/A
AAV5-hSyn::DIO-hM4Di-mCherry	Addgene	# 44362
ENV-Rb-ΔG-eYFP	Kavli institute	N/A
Chemicals, peptides, and recombinant proteins		
Acrylamide	bio-rad	#161-0140
Bisacrylamide	bio-rad	#161-0142
VA-044 initiator	Wako	011-19365
Boric acid	sigma	#B7901
Tris base	Bio-lab	002009239100
sodium dodecyl sulfate (SDS)	sigma	#L3771
tritonX100	ChemCruz	#sc-29112A
CLARITY Specific Rapiclear	SunJin lab	#RCCS002
Clozapine *N*-oxide (CNO)	Tocris Bioscience	#4936
4 hydroxytamoxifen (4-OHT)	Sigma	H7904
Deposited data		
Raw data	Mendeley	https://doi.org/10.17632/9x9xph4v46.1
Experimental models: Organisms/strains		
B6;129S6-Gt(ROSA)26Sor$^{tm14(CAG-tdTomato)Hze}$	Jackson laboratory	J-Stock No: 007908; RRID:IMSR_JAX:007908
Fos$^{tm2.1(icre/ERT2)Luo}$	Jackson laboratory	J-Stock No: 030323; RRID:IMSR_JAX:030323
Software and algorithms		
EthoVision tracking software version 13	Noldus	N/A
Olympus Fluoview Viewer version 4.2	Olympus	N/A
Bitplane IMARIS 9.1.2	Bitplane	N/A
SyGlass	IstoVisio	N/A
MATLAB 2018	MathWorks	N/A
IBM SPSS statistics	IBM Analytics	N/A

RESOURCE AVAILABILITY

Lead contact

Further information and requests for resources and reagents should be directed to and will be fulfilled by the lead contact, Inbal Goshen (inbal.goshen@elsc.huji.ac.il).

Material availability

This study did not generate new unique reagents.

Data and code availability

- All data reported in this paper will is shared in the following DOI: https://doi.org/10.17632/9x9xph4v46.1.
- All original code is available upon request.
- Any additional information required to reanalyze the data reported in this paper is available from the lead contact upon request.

EXPERIMENTAL MODEL AND STUDY PARTICIPANT DETAILS

Male Ai14 or TRAP2 mice were group housed on a 12 hr light/dark cycle with *ad libitum* access to food and water. All mice were maintained under pathogen-free conditions in IVC, GM400 cages (Tecniplast) bedding, at 20-24°C, and fed Teklad 2918SC (ENVIGO) pellets. Mice were randomly assigned to experimental groups. Experimental protocols were approved by the Hebrew University Animal Care and Use Committee and met the guidelines of the National Institute of Health guide for the Care and Use of Laboratory Animals.

METHOD DETAILS

Stereotactic Injections

Mice were anesthetized with isoflurane, and their heads were placed in a stereotactic apparatus (Kopf Instruments, USA). The skull was exposed and a small craniotomy was performed. Mice were bilaterally microinjected using the following coordinates - for the CA1: Anteroposterior (AP), -1.85mm from Bregma, Mediolateral (ML), ±1.4mm, Dorsoventral (DV), -1.5mm. For the ACC: AP +0.35mm, ML ±0.35mm, DV -1.8mm. For the NAc: AP -1.2mm, ML ±1.1mm, DV -4.5mm. All microinjections were performed using a 10μL syringe and a 34-gauge metal needle (WPI, Sarasota, USA). The injection volume and flow rate (0.1 ml/min) were controlled by an injection pump (WPI). Following each injection, the needle was left in place for 10 additional minutes to allow for diffusion of the viral vector away from the needle track and was then slowly withdrawn. The incision was closed using sewing and Vetbond tissue adhesive. For postoperative care, mice were subcutaneously injected with Tramadex (5mg/kg).

Viral Vectors

AAV5-cFos::creER, AAVretro-CaMKII::iCre, AAVretro-CaMKII::GFP, AAV2-CAG::flex-TC66T-mCherry, AAV2-CAG::flex-oPBG were all from the ELSC Vector Core Facility. AAV5-hSyn::DIO-hM4Di-mCherry was purchased from Addgene (# 44362).

ENV-Rb-ΔG-eYFP was purchased from the viral vector core at the Kavli institute in Norway.

4-hydroxytamoxifen (4-OHT)

4-OHT was freshly prepared every day, and administered (i.p.) one hour after the relevant memory related task, when blood concentration peaks, to enable CreER-mediated recombination. The 4-OHT solution was prepared with the following ratios: For Ai14 mice (25mg/kg), 3 mg of 4-OHT (Sigma H7904) were dissolved in 120μl of ethanol, and 480μl of sunflower oil. For TRAP mice (75mg/kg), 9 mg of 4-OHT were dissolved in 120μl of ethanol, and 480μl of sunflower oil.

CNO administration

IP injections: CNO (Tocris #4936) was dissolved in DMSO and then diluted in 0.9% saline to yield a final DMSO concentration of 0.5%. Saline solution for control injections also consisted of 0.5% DMSO. 10mg/kg CNO was intraperitoneally injected 30min before the behavioral assays for the Gi pathway activation of the recent engram neurons. The chosen doses of CNO did not induce any behavioral signs of seizure activity.

CNO in drinking water: For chronic inhibition of the CA1→ACC, 70mg CNO were dissolved in 1ml of DMSO and added together with 10ml sucrose to 1L of water. A single IP injection of 10mg/kg CNO was administered immediately after recent recall, followed by the same concentration in their drinking water. The control group received the same ingredients (DMSO, sucrose) without the CNO. Drinking bottle was protected from light and replaced every 24 hours to ensure 10mg/kg/day.

Fear Conditioning

The fear conditioning apparatus consisted of a conditioning cage with a grid floor wired to a shock generator and surrounded by an acoustic chamber. To induce fear conditioning, mice were placed in the cage for two minutes, and a pure tone (2.9 kHz) was then sounded for 20 seconds followed by a two second foot shock (0.6mA). This procedure was then repeated, and 30 seconds after the delivery of the second shock, mice were extracted from the conditioning cage. Fear was assessed by a continuous measurement of freezing (complete immobility), the dominant behavioral fear response. To test contextual fear conditioning, mice were placed in the original conditioning cage, and freezing was measured for five minutes. Contextual fear conditioning recall was measured at day 1, day 2, day 4, day 15, day 28, and day 30, depending on the group to which the mouse was assigned.

Immunohistochemistry

90 minutes after the last memory task, mice were transcardially perfused with cold PBS followed by immediate removal of the brain into 4% paraformaldehyde (PFA) in phosphate-buffered saline (PBS). Brains were postfixed overnight at 4°C and cryoprotected in

30% sucrose in PBS. Brains were sectioned to a thickness of 50 μm using a sliding freezing microtome (Leica SM 2010R) and preserved in a cryoprotectant solution (25% glycerol and 30% ethylene glycol in PBS). Free-floating sections were washed in PBS, incubated for 1 hr in blocking solution (1% of bovine serum albumin, BSA, and 0.3% Triton X-100 in PBS). For cFos staining, the relevant brain slices were incubated for 7 days at 4°C with rabbit anti-cFos primary antibody (Synaptic system, #226003), and for the mCherry staining, slices were incubated overnight at 4°C with rabbit anti-mCherry primary antibody (Invitrogen, #PA5-34974). Sections were then washed with PBS and incubated for 2 hr at room temperature with secondary antibody (1:500, AF 647, donkey anti rabbit, #711-605-152, Jackson laboratory) in 1% BSA in PBS. Finally, sections were washed in PBS, incubated with 4,6-diamidino-2-phenylindole (DAPI; Sigma 1μg ml-1), and mounted on slides with Mounting Medium (Dako, #S3025).

CLARITY

Full hemispheres were cleared based on a modified protocol[55] derived from that described by Ye et al..[26] Briefly, >12 weeks old mice were transcardially perfused with ice cold PBS followed by 4% PFA, brains were removed and kept in 4% PFA overnight at 4°C. Brains were then transferred to a 2% hydrogel solution (PBS with: 2% acrylamide, bio-rad #161-0140; 0.1% Bisacrylamide, bio-rad #161-0142; 0.25% VA-044 initiator, Wako, 011-19365; 4% PFA) for 48 hr. The samples were then degassed with N2 for 45 min and polymerized in 37°C for 3.5 hr. After degassing, the samples were cut at the mid-sagittal plane. The samples were then washed overnight in 200 mM NaOH-Boric buffer (sigma, #B7901) containing 8% sodium dodecyl sulfate (SDS) (sigma, #L3771), to remove PFA residuals. Samples were then stirred in a clearing solution (100 mM Tris-Boric buffer, bio-lab, #002009239100 with 8% SDS) at 37°C for 3–4 weeks. After the samples became transparent, they were washed with PBST (PBS with 0.5% tritonX100; ChemCruz, #sc-29112A) for 48 hr at 37°C with mild shaking (replacing the PBST every 24 hr) and for another 24 hr with new PBST 0.5% at RT. Finally, the samples were incubated in the refractive index matched solution CLARITY Specific Rapiclear (RI = 1.45; SunJin lab, #RCCS002) O/N at 37°C and for two more days at room temperature before imaging.

Transparent samples were embedded onto a slide surrounded by hot-glue walls. Thin coverslip glass was the placed over the brain from above, closing all exits. CLARITY specific RapiClear solution was then inserted into the chamber, covering the entire brain. Our expanded protocol can be found in JoVE.[56]

Confocal Imaging

Confocal fluorescence images were acquired using an Olympus scanning laser microscope Fluoview FV1000 using 4X and 10X air objectives, 10X, and 20X water immersion objectives or 20X oil immersion objectives. Images were created by imaging between 30μm-5000μm in depth and reconstructing them using IMARIS 9.1.2 software (Bitplane, UK).

Imaris analysis

A number of brain slices were imaged per mouse. Using the 'spot' feature on the Imaris software, (x,y) coordination were manually counted and extracted for all marked cells, DAPI included. To calculate the percentage of expected overlap between two groups out of a specific group, for each slice, the number of cells in the relevant group was divided by the number of the total amount of cells (i.e. DAPI), and multiplied by the same division for the second group in order to estimate the percentage expected overlap. This number was then multiplied by DAPI in order to predict the number of estimated overlap cells, and later divided by the number of counted cells of the first group in order to estimate the percentage of overlap cells out of the relevant group. Finally, the percentage of actual overlap cells were calculated by dividing the empirical number of overlap cells by the number of counted cells of the first group. This parameter was later divided by the expected overlap, allowing us to calculate the fold from expected measurement:

$$\frac{\frac{amount\ of\ counted\ x\ and\ y}{amount\ of\ counted\ x}}{\frac{amount\ of\ counted\ x}{DAPI} * \frac{amount\ of\ counted\ y}{DAPI} * DAPI}{amount\ of\ counted\ x}$$

where 'x' represents the sub group of cells from which we wanted to extract the percentage (i.e. 'how many of x cells were also y cells, out of the total amount of x cells').

All counting was done by the same individual, using a Matlab code to find overlapped cells.

QUANTIFICATION AND STATISTICAL ANALYSIS

Data is presented as mean ± standard error of the mean (SEM) unless otherwise indicated in figure legends. Sample number (n) indicates the number of slices or mice in each experiment and is specified in the figure legends and in the results suction. Results were analyzed by Student's t test, paired t-test or one-way ANOVA, followed by Tukey post hoc tests, as applicable. All the statistical details of experiments can be found in the result section. Differences in means were considered statistically significant at $p < 0.05$. Analyses were performed using the IBM SPSS Statistics or Matlab software. Subjects were excluded from analysis when they deviated by more than two standard deviations from the mean.